



The Mitochondrial Targets of Neuroprotective Drug Vinpocetine on Primary Neuron Cultures, Brain Capillary Endothelial Cells, Synaptosomes, and Brain Mitochondria

Gergely Svab¹ · Judit Doczi¹ · Akos A. Gerencser^{1,2} · Attila Ambrus¹ · Ferenc Gallyas^{3,4,5} · Balazs Sümegi^{3,4,5} · László Tretter¹

Received: 29 August 2019 / Revised: 29 August 2019 / Accepted: 5 September 2019 / Published online: 18 September 2019
© The Author(s) 2019

Abstract

Vinpocetine is considered as neuroprotectant drug and used for treatment of brain ischemia and cognitive deficiencies for decades. A number of enzymes, channels and receptors can bind vinpocetine, however the mechanisms of many effects' are still not clear. The present study investigated the effects of vinpocetine from the mitochondrial bioenergetic aspects. In primary brain capillary endothelial cells the purinergic receptor-stimulated mitochondrial Ca^{2+} uptake and efflux were studied. Vinpocetine exerted a partial inhibition on the mitochondrial calcium efflux. In rodent brain synaptosomes vinpocetine (30 μM) inhibited respiration in uncoupler stimulated synaptosomes and decreased H_2O_2 release from the nerve terminals in resting and in complex I inhibited conditions, respectively. In isolated rat brain mitochondria using either complex I or complex II substrates leak respiration was stimulated, but ADP-induced respiration was inhibited by vinpocetine. The stimulation of oxidation was associated with a small extent of membrane depolarization. Mitochondrial H_2O_2 production was inhibited by vinpocetine under all conditions investigated. The most pronounced effects were detected with the complex II substrate succinate. Vinpocetine also mitigated both Ca^{2+} -induced mitochondrial Ca^{2+} -release and Ca^{2+} -induced mitochondrial swelling. It lowered the rate of mitochondrial ATP synthesis, while increasing ATPase activity. These results indicate more than a single mitochondrial target of this vinca alkaloid. The relevance of the affected mitochondrial mechanisms in the anti ischemic effect of vinpocetine is discussed.

Keywords Vinpocetine · Neuroprotection · Mitochondria · Reactive oxygen species · Calcium induced calcium release · Oxygen consumption · ATP synthesis · Uncoupling

Balazs Sümegi: Deceased on Aug 1, 2019.

Special issue In honour of Professor Vera Adam-Vizi.

The authors dedicate this article to Prof. Vera Adam-Vizi as an appreciation for her all time support, encouragement, positive criticism, and high expectations.

✉ László Tretter
tretter.laszlo@med.semmelweis-univ.hu

¹ Department of Medical Biochemistry, MTA-SE Laboratory for Neurobiochemistry, Semmelweis University, 37-47 Tuzolto Street, Budapest 1094, Hungary

² Buck Institute for Research on Aging, Novato, CA, USA

Introduction

Vinpocetine has been marketed for more than 30 years. Among its indication are ischemic neuronal damage [1], stroke [2, 3], cerebrovascular diseases [4], neurodegenerative diseases [5, 6], dementia and cognitive deficits [1, 7]. During this period many targets and mechanisms of actions has been proposed, including the inhibition of the cyclic nucleotide phosphodiesterase 1 (PDE1) [8, 9], voltage-dependent Na^+

³ Department of Biochemistry and Medical Chemistry, University of Pecs Medical School, Pecs, Hungary

⁴ Szentagothai Research Centre, University of Pecs, Pecs, Hungary

⁵ Nuclear-Mitochondrial Interactions Research Group, Hungarian Academy of Sciences, Budapest, Hungary

channels [10, 11], the I κ B kinase, the NF- κ B [12] and binding to peripheral benzodiazepine receptors [13]. For a recent review see [14]. As a consequence of having numerous targets, the drug can influence diverse functions. The present study focuses on the effects of vinpocetine on mitochondrial function. The brain is extremely sensitive to proper provision of energy, in which mitochondria play a central role. Most of the inborn errors of metabolism are associated with structural and/or functional brain damage and mental retardation. Mitochondria are not only cellular power stations, but also pollute their environment with reactive oxygen species (ROS). Although as a consequence of powerful antioxidant systems most of the mitochondrially produced ROS will not leave the mitochondria in physiological conditions [15], excessive mitochondrial ROS generation is considered as an important factor in cerebral ischemia/reperfusion injury [16–19], neurodegeneration [20] and glutamate toxicity [21, 22]. Early studies already addressed mitochondria as potential vinpocetine targets, but only in a very few studies were mitochondria the focus of the investigation. Vinpocetine's effect has been explained by binding to the peripheral benzodiazepine receptor [22], a mitochondrial outer membrane protein and putative component of the mitochondrial permeability transition pore (PTP). In the present study the effects of vinpocetine are investigated at three level of complexity, in cellular systems (primary neuronal and endothelial cell cultures), in isolated nerve terminals (synaptosomes) and in isolated guinea pig brain mitochondria. Complex biological phenomena like delayed calcium deregulation, intracellular calcium transients and Ca²⁺ release from in situ mitochondria have been investigated in cellular systems, while mitochondrial oxygen consumption, ROS production, ATPase activity in isolated mitochondria. We conclude that the delayed PTP opening, mild mitochondrial depolarization and decreased H₂O₂ release may all play an important role in the beneficial effects of vinpocetine in pathological conditions associated with neuronal damage.

Materials and Methods

Animals

For cell culture and synaptosomal experiments Wistar rats were used. Mitochondria were isolated from guinea pig brain. Animal experiments were performed in accordance with the Guidelines for Animal Experiments at Semmelweis University.

Cell Cultures

Brain capillary endothelial cells from 3 to 5 month-old Wistar rats were prepared and seeded on extracellular

matrix coated glass coverslips as described earlier [23]. Cultures were kept in DMEM containing 17% plasma-derived bovine serum (First Link, UK), supplemented with 2 mM glutamine, 80 μ g/ml heparin, 150 μ g/ml endothelial cell growth supplement (Sigma), antibiotics, and trace factors (vitamin C, selenium, insulin, transferrin and glutathione). After reaching confluence, experiments were performed on 6–10 days old primary cultures.

Primary neuron-enriched cultures were prepared from E17 Wistar rat embryos, plated on 6 mm glass coverslips coated with poly-L-ornithine plus laminin in 12-well plates or on Petri dishes coated with poly-D-lysine, and maintained in Neurobasal medium (Invitrogen, Carlsbad, CA) with 2% B27 supplement (Invitrogen) and 2 mM glutamine for 8–12 days at 37 °C, 5% CO₂ without feeding [24].

Measurements of Mitochondrial Calcium Transients

In situ mitochondrial and cytoplasmic calcium measurements were performed in brain capillary endothelial cell cultures (at 7–8 days in vitro) by X-Rhod-1-AM (Molecular Probes, Eugene, OR, USA), localized mainly in mitochondria, a calcium sensitive dye with fluorescence microscopy as described earlier [25]. Briefly, mitochondrial calcium transients ($[Ca^{2+}]_m$) were analyzed using highpass spatial filtering of fluorescence images using the “the original X-rhod-1 mito filter.flt” in Image Analyst MKII (Image Analyst Software, Novato, CA, USA). Cytosolic calcium transients ($[Ca^{2+}]_c$) were analyzed on the same images left unfiltered by the measurement of X-Rhod-1 fluorescence of the nuclear region in the cell [25]. Half decay time ($\tau_{1/2}$) was defined as the time between peak of the transient and the intensity decaying to half of the peak amplitude.

Fluorimetric measurements were performed to examine potential optical or chemical interaction of vinpocetine and calcium sensitive fluorescent dyes (X-Rhod-1 and Fura-FF), to exclude the possibility of recording artefacts due to the change in fluorescence. Fluorescence of vinpocetine in aqueous solution was negligible both in the range of Fura-FF emission 510 nm (excitation: 340/380 nm) and in the range of X-Rhod-1 emission 570 nm (excitation: 535 nm). 30 μ M vinpocetine had no effect on the fluorescence of hydrolyzed X-Rhod-1 or Fura-FF dyes either in high calcium (40 μ M) containing or in calcium free intracellular solution (pH 7.4, 37 °C).

Measurement of Delayed Ca²⁺ Deregulation in Isolated Primary Rat Brain Neurons

Time-lapse fluorescence microscopy of rat primary cortical cultures was carried out using the above fluorescence

microscope setup using a UAPO 20× dry 0.75 NA lens. Cultures were incubated with Fura-FF-AM (3 μM) for 15 min at 37 °C and subsequently rinsed with superfusion medium. Fura-FF fluorescence was ratio imaged using 340/10 (center/bandwidth in nm) and 380/10 excitors (Chroma, Rockingham, VT, USA), a 400DCLP dichroic mirror and a 470LP long pass emitter (Omega Optical, Brattleboro, VT, USA) [24].

Isolation of Synaptosomes from Rat Brain

Synaptosomes were isolated from rat brain cortex as described earlier [26]. The synaptosomal fraction was obtained after sucrose (0.8 M) gradient centrifugation. Sucrose was diluted by ice cold distilled water to 0.32 M and synaptosomes were sedimented with 20,000×g for 20 min. The pellet's protein concentration was adjusted to about 20 mg/ml, and synaptosomes were kept on ice until use.

Most of the experiments were performed in standard extracellular medium composed of (mM): 140 NaCl, 3 KCl, 2 MgCl₂, 2 CaCl₂, 10 PIPES pH 7.38 and 10 glucose. Incubations and measurements were done at 37 °C. Synaptosomes retained their basic bioenergetic parameters for at least 6 h.

Isolation of Rodent Brain Mitochondria

Guinea pig mitochondria were isolated using discontinuous percoll gradient as described [27]. Mitochondria were incubated in the following incubation buffer (mM): 125 KCl, 20 HEPES, 2 K₂HPO₄, 1 MgCl₂, 0.1 EGTA, at pH 7.0 adjusted by KOH. Incubation buffer was supplemented with 0.025 w/v % fatty acid free BSA. To use BSA was necessary, because mitochondria may lose their functional parameters very quickly as a consequence of liberated fatty acids [28].

Oxygen Consumption of Synaptosomes and Mitochondria

Oxygen consumption of synaptosomes were measured by high resolution respirometry Oxygraph-2K (Oroboros Instruments, Innsbruck, Austria) [29] at 37 °C in 2-ml chambers. Data were digitally recorded and analyzed; oxygen flux was calculated as the negative temporal derivative of the oxygen concentration, $cO_2(t)$. Oxygen sensors were calibrated routinely in air saturated and oxygen depleted media. Synaptosomal protein concentration was 2 mg/ml, mitochondrial protein concentration was 0.1 mg/ml.

Measurement of Mitochondrial Membrane Potential ($\Delta\Psi_m$)

Mitochondrial membrane potential was measured by a custom-made tetraphenylphosphonium (TPP⁺) electrode [30]. TPP⁺ is a lipophilic membrane permeable cation. With the TPP⁺ electrode the extramitochondrial concentration of TPP⁺ was measured as described earlier. Knowing the total concentration of the TPP⁺ $\Delta\Psi_m$ was calculated using the Nernst equation.

Measurement of H₂O₂ Production in Mitochondria and in Synaptosomes

H₂O₂ released from mitochondria was detected with horseradish peroxidase (5U/2 ml) and Amplex Ultrared (3 μM) [31]. As a result of peroxidase action Amplex Ultrared was converted to fluorescent resorufin in the presence of mitochondria (0.1 mg/ml), and measured using PTI Deltascan fluorescence spectrophotometer (550 nm excitation, 585 nm emission wavelengths; Photon Technology International, Lawrenceville, NJ, USA). Each measurement was calibrated with known amounts of H₂O₂ at the end of the experiment.

Measurement of Mitochondrial Ca²⁺ Uptake

Mitochondria (0.05 mg/ml) were incubated in the following reaction medium (mM): 8 KCl, 110 K-gluconate, 10 NaCl, 10 HEPES, 2 KH₂PO₄, 4 MgCl₂, 10 mannitol, 5 glutamate, 5 malate, 3 ATP, 0.25 ADP pH 7.25 (KOH) supplemented with 0.025% BSA. The free Ca²⁺ concentration was calculated with the WinMAXC software ([32, 33]. Ca²⁺ (CaCl₂) was given to mitochondria in the form of 12.5 μM Ca²⁺ pulses. The Ca²⁺ level of the medium was followed by Calcium-Green 5 N (K_D = 4.29 μM). Wavelengths for Calcium-green fluorescence were 505 nm excitation and 535 nm emission, respectively.

Measurement of Mitochondrial Swelling

Swelling of isolated mitochondria can reflect permeability pore opening (see [33, 34]) and was followed by light scattering at 590 nm in parallel with mitochondrial Ca²⁺ uptake using double excitation, double emission mode of PTI Deltascan spectrofluorimeter. At the end of each measurement alamethicin (a pore forming peptide 80 μg/2 ml) was added to obtain maximal swelling.

Kinetic measurement of Mitochondrial ATP Synthesis

Mitochondrial ATP formation was monitored by a combined enzymatic system comprising of hexokinase and

glucose-6-phosphate dehydrogenase, as described earlier [35, 36]. Mitochondria (0.05 mg/ml) were incubated in the medium described in the isolation procedure. This medium was supplemented with 3 mM NADP^+ , 1.5 U hexokinase, 0.5 U glucose-6-phosphate dehydrogenase, 5 mM glucose, 2 mM ADP and 200 μM AP5 (P^1, P^5 -Di(adenosine-5') pentaphosphate, an inhibitor of adenylate kinase) in 2 ml total volume (Melnick et al. 1979). In the presence of mitochondria, ADP and respiratory substrates glutamate *plus* malate ATP was formed, which mostly left the mitochondria via the adenine nucleotide translocase. ATP phosphorylated glucose (to glucose-6-phosphate) by hexokinase. The resulted product glucose-6-phosphate was oxidized to 6-phosphogluconate by glucose-6-phosphate dehydrogenase with the concomitant reduction of NADP^+ to NADPH. Thus, NADPH formation was stoichiometrically equal to ATP released from the mitochondria. The absorbance of NADPH ($\epsilon = 6220 \text{ M}^{-1} \text{ cm}^{-1}$) was recorded at 340 nm, 37 °C using a JASCO V-650 spectrophotometer (ABL&E-JASCO, Tokyo, Japan). ATP standards were used for calibration.

Measurement of ATPase Activity

ATP hydrolyzed by mitochondria in the absence of respiratory substrates was measured by a combined enzyme assay [37]. The standard assay medium was supplemented with NADH (300 μM), lactate dehydrogenase (2 U/ml),

pyruvate kinase (PK; 2 U/ml), phosphoenolpyruvate (PEP; 2 mM), ATP (0.5 mM), and rotenone (1 μM). In the medium, ADP was phosphorylated to ATP in the presence of PK and PEP, then pyruvate was reduced to lactate with the concomitant oxidation of NADH to NAD^+ . Absorbance of NADH was monitored at 340 nm using a JASCO spectrophotometer. Measurements were calibrated with known amounts of ADP.

Statistics

Statistical differences were evaluated with ANOVA in Sigmatstat wherever multiple comparisons were made. Values are indicated as mean \pm standard error, $p < 0.05$ were considered statistically significant.

Results

In Situ Mitochondrial Ca^{2+} Measurements in Brain Capillary Endothelial Cells

Brain capillary endothelial cells in primary culture were stimulated by the application of 100 μM ATP (Fig. 1). ATP triggers a transient rise of cytoplasmic $[\text{Ca}^{2+}]_c$ (Fig. 1b) and mitochondrial $[\text{Ca}^{2+}]_m$ (Fig. 1a) by activating purinergic receptors and IP₃-mediated Ca^{2+} release from the endoplasmic reticulum [23]. Mitochondria take up Ca^{2+} from the cytoplasm by the calcium

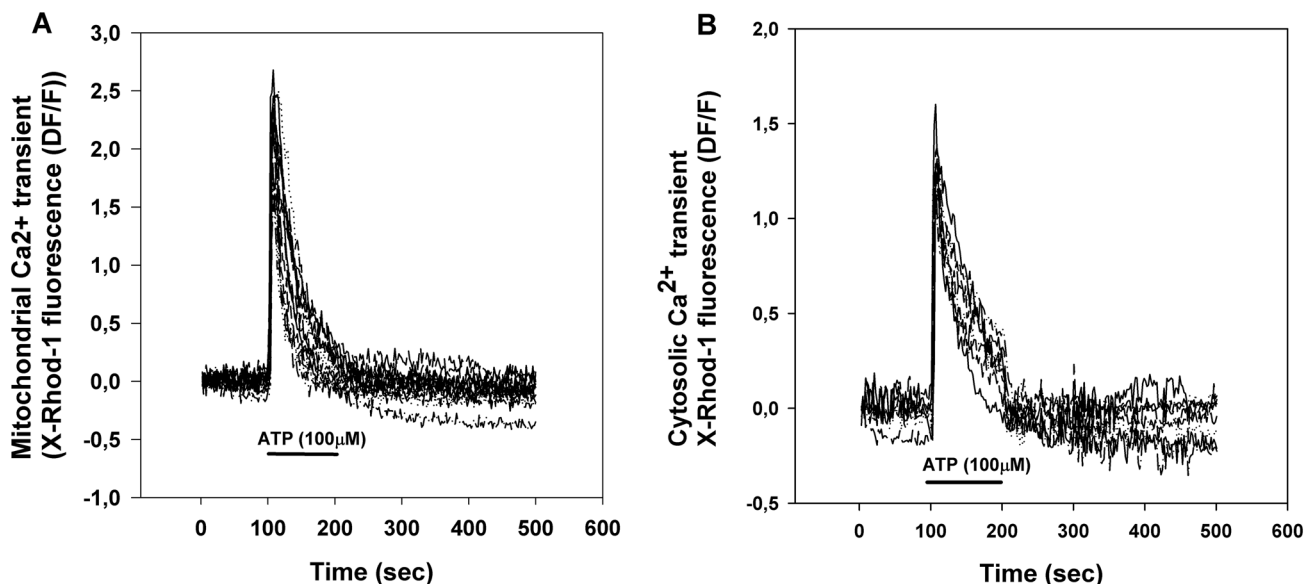


Fig. 1 Mitochondrial (a) and cytosolic (b) calcium transients of primary brain capillary endothelial cells stimulated by the addition of 100 μM ATP. ATP was provided by superfusion at the indicated time.

Mitochondrial and cytosolic Ca^{2+} transients were extracted from the same recordings using image processing. Pooled from 3 measurements, total cell number: 17

uniporter any Ca^{2+} is predominantly released from mitochondria by the $\text{Na}^+/\text{Ca}^{2+}$ exchanger.

In the stimulation paradigm depicted in Fig. 1, any change to Ca^{2+} ‘handling’ in mitochondria is indicated by the alteration of the peak amplitude or the half decay time of the mitochondrial Ca^{2+} transient. Alteration of the peak amplitude indicates changes both in the calcium influx and efflux while alteration of half decay time indicates change in the calcium efflux.

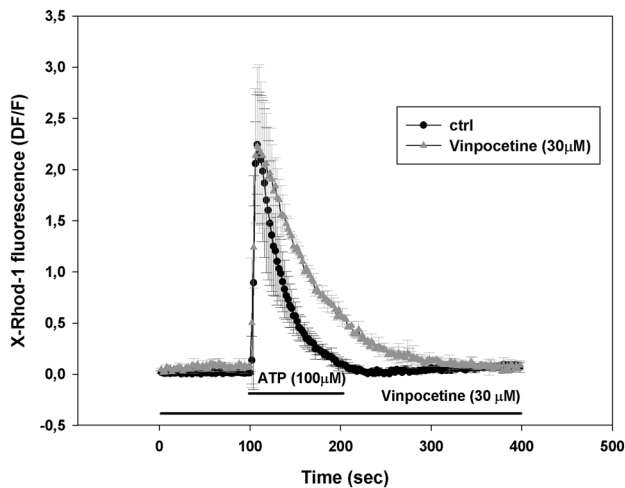


Fig. 2 Effect of Vinpocetine (30 μM) pretreatment on the mitochondrial calcium transient. Data are expressed as mean \pm SE of $n=3$ experiments; ctrl, untreated control in matched culture preparations

Effect of Vinpocetine on ATP Induced $[\text{Ca}^{2+}]_m$ and $[\text{Ca}^{2+}]_c$ Transients

Vinpocetine up to 10 μM had no significant effects on the parameters of $[\text{Ca}^{2+}]_m$, or $[\text{Ca}^{2+}]_c$ transients (not shown). However, 30 μM vinpocetine pretreatment significantly increased half decay time of the mitochondrial calcium transient (from $\tau_{1/2} = 23.5 \pm 6.8$ s to 42 ± 6.2 s, $p < 0.05$), but peak amplitude was not changed (from amplitude 2.24 ± 0.48 to 2.22 ± 0.77 ; given as relative fluorescence change from baseline, $\Delta F/F_0$) (Fig. 2).

Parameters of the cytosolic calcium transients were not significantly different (from $\tau_{1/2} = 33.3 \pm 5.2$ s to $\tau_{1/2} = 29 \pm 8.69$ s and from amplitude 1.33 ± 0.13 to 1.53 ± 0.15). Figure not shown.

The Effect of Vinpocetine on Delayed Ca^{2+} Deregulation (DCD)

DCD is a model of glutamate toxicity, where excessive calcium load through Ca^{2+} permeable glutamate receptors could result in deterioration of calcium and energy homeostasis and eventually lead to cell death [38]. Primary cortical neurons were stimulated with glutamate (300 μM) plus glycine (10 μM) for 20 min in Mg^{2+} -free solution and cytoplasmic $[\text{Ca}^{2+}]$ was measured using a low affinity calcium-sensitive fluorescent dye Fura-FF in single cells. The glutamate-induced initial Ca^{2+} peak was followed by a transient plateau where the cytosolic $[\text{Ca}^{2+}]$ remained lower than the peak, but higher than before the stimulation. The length of this period had large cell to cell variations

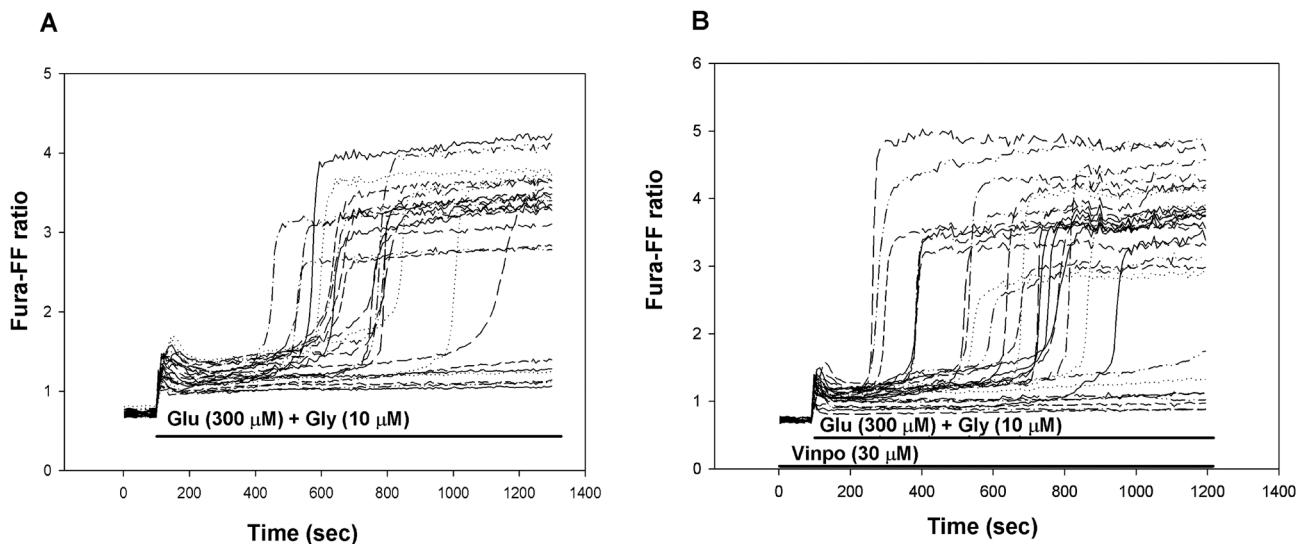


Fig. 3 Delayed Ca^{2+} deregulation in primary cortical neurons in the absence (a) or presence (b) of vinpocetine (30 μM). Glutamate plus glycine (Glu + Gly) (a, b) and vinpocetine (vinpo) (b) were applied as

indicated. The Fura-FF fluorescence excitation ratio reflects the cytosolic Ca^{2+} levels. Representative traces are shown

and was followed by a sharp, irreversible elevation of $[Ca^{2+}]_c$ termed as DCD (Fig. 3a). Vinpocetine pretreatment (Fig. 3b) was unable to protect cells against DCD. There was neither a change in the mean time of DCD, nor in the fraction of cells exhibiting DCD within the time-frame of the experiment (20 min).

The Effects of Vinpocetine on Synaptosomal Oxygen Consumption

Oxygen consumption of synaptosomes reflects substrate oxidation by in situ synaptosomal mitochondria, whereas contaminating, free mitochondria are assumed to be damaged and metabolically silent in the presence of mM extracellular Ca^{2+} . Vinpocetine inhibited both resting and uncoupler-stimulated respiration of nerve endings, energized by glucose (Fig. 4). Replacing glucose by lactate resulted in similar results (data not shown).

Effects of Vinpocetine on Synaptosomal H_2O_2 Production

In synaptosomes, ROS production can primarily be attributed to mitochondria. To address the effects of vinpocetine on ROS generation, cortical synaptosomes supplied with glucose were preincubated with vinpocetine (10 or 30 μM) for 5 min. Vinpocetine lowered H_2O_2 release by 22%. In the presence of the complex I inhibitor rotenone-vinpocetine also significantly decreased H_2O_2 production by 19.7% (Fig. 5).

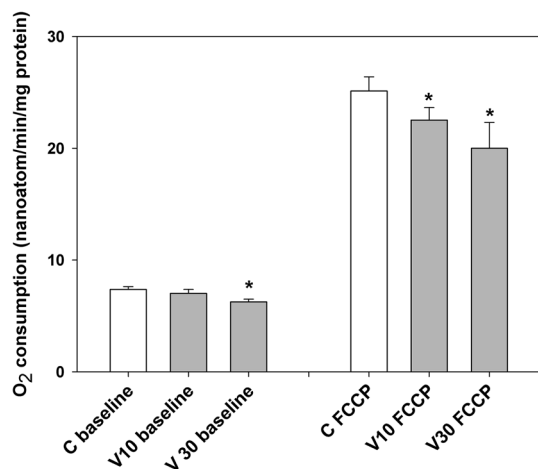


Fig. 4 The effect of vinpocetine on the O_2 consumption of synaptosomes. Synaptosomes were preincubated in glucose containing standard medium for 5 min under control conditions (C, white bars), or in the presence of vinpocetine (V, grey bars, 10 or 30 μM). First basal respiration (C baseline, V10 baseline, V30 baseline) was measured and then respiration was stimulated by the uncoupler FCCP (500 nM, C FCCP, V10 FCCP, V30 FCCP). * indicate significant difference ($p < 0.05$, $n > 4$) from the corresponding control measured in the absence of vinpocetine

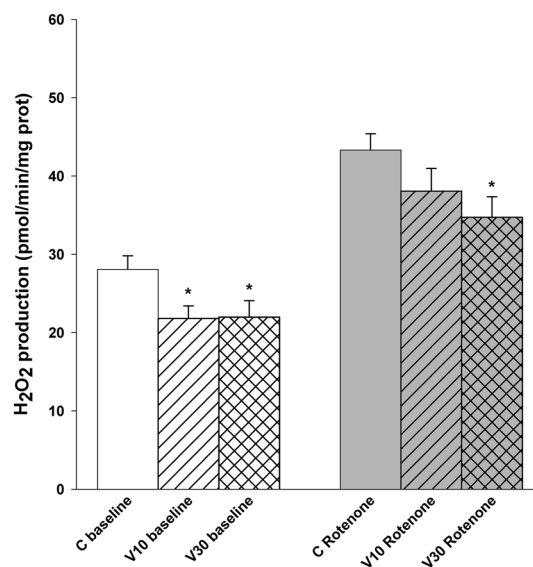


Fig. 5 Effect of vinpocetine on H_2O_2 production of synaptosomes. Synaptosomes were preincubated in glucose-containing standard medium for 5 min under control conditions (C) or with vinpocetine (10 or 30 μM , hatched and cross hatched bars). Recording of baseline H_2O_2 formation was started after addition of Amplex Ultrared and horseradish peroxidase. After 200 s rotenone (1 μM , gray bars) was given. * indicate significant difference ($p < 0.05$, $n > 4$) compared to the corresponding control measured in the absence of vinpocetine

Effects of Vinpocetine on Mitochondrial Membrane Potential

In isolated guinea pig brain mitochondria $\Delta\psi_m$ was measured with TPP⁺-electrode. Mitochondria were energized either by glutamate *plus* malate or succinate. After the development of $\Delta\psi_m$ vinpocetine (30 μM) was given. Vinpocetine decreased $\Delta\psi_m$ in glutamate *plus* malate supported mitochondria by 4.0 ± 0.6 mV. In succinate supported mitochondria similar depolarization was detected (data not shown).

Effects of Vinpocetine on the Respiration of Isolated Guinea Pig Brain Mitochondria

Isolated mitochondria are intact cellular organelles with complex bioenergetic functions, e.g. membrane potential, ATP synthesis and Ca^{2+} transport. Brain mitochondria were supported with complex I (glutamate *plus* malate) or complex II (succinate) substrates. Adding vinpocetine during resting respiration (state 2, substrate only) stimulated oxygen consumption. In contrast in the presence of ADP (state 3 respiration) the rate of oxygen consumption was decreased by vinpocetine irrespective of the substrates applied (Fig. 6). Similarly, if vinpocetine was added after ADP, there was an immediate decrease in the respiration rate

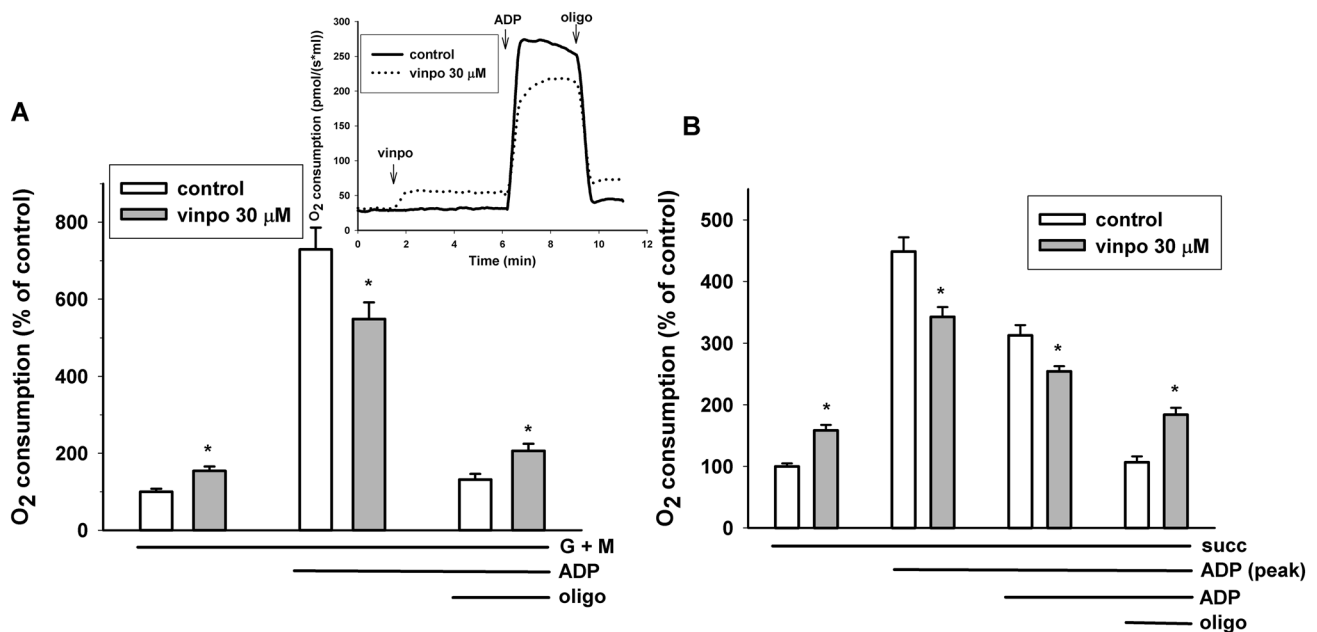


Fig. 6 Effects of vinpocetine on mitochondrial respiration. Mitochondria supported by glutamate *plus* malate respiratory substrates (a) or by succinate (b) were incubated in standard mitochondrial medium. Vinpocetine (vinpo; 30 μM), ADP (2 mM) and oligomycin (oligo; 5 μM) were added as indicated in the original traces of the inset. The

effects of vinpocetine (gray bars) were compared to the control (white bars, vehicle treated). Data are % of mean control oxygen consumption. Mean ± SE; n > 5; * significant difference from the corresponding solvent controls

(not shown). Addition of oligomycin decreased the rate of respiration, but in the presence of vinpocetine the remaining respiration rate (leak respiration) was always higher than under control conditions, indicating the uncoupling effect of this vinca derivative.

Effects of Vinpocetine on H₂O₂ Formation in Isolated Mitochondria

Usually there is a close correlation between the rate of oxidation and H₂O₂ production. The mitochondrial H₂O₂ formation has been investigated with glutamate *plus* malate and succinate substrates.

Using the complex I substrates glutamate *plus* malate, basal ROS production was only a fraction of that detected in succinate-supported mitochondria. This observation agrees with our and others previous studies [39, 40]. Vinpocetine also decreased the rate of H₂O₂ formation in the presence of glutamate *plus* malate (Fig. 7). Stimulation of respiration with ADP resulted in a decrease of ROS production irrespective of the presence or absence of vinpocetine. Inhibition of ATP synthesis with oligomycin stimulated H₂O₂ formation, and this increase was more modest (201% vs. 387%) in vinpocetine-treated mitochondria (Fig. 7a).

In succinate supported mitochondria ROS production was 2074 ± 282 pmol/min/mg protein. Under control conditions ADP dramatically decreased ROS production by 94.6%. Vinpocetine added after succinate decreased H₂O₂ formation by 79.4%. Addition of the ATP synthesis inhibitor oligomycin stimulated H₂O₂ release by a factor of 22.2, while in the presence of vinpocetine only by a factor of only 6.1 (Fig. 3b).

ATP Synthesis in Mitochondria

The most important bioenergetic function of mitochondria is ATP production. Alterations in state 3 respiration and membrane potential suggested a decreased capacity for ATP production. Measurement of ATP release from mitochondria in the presence of respiratory substrates and ADP provides information about this complex function.

Mitochondrial ATP synthesis was measured in glutamate *plus* malate supported mitochondria. In the presence of glutamate *plus* malate vinpocetine evoked a dose-dependent inhibition of ATP synthesis (Fig. 8a). Applying 30 μM vinpocetine decreased ATP production by $17.9 \pm 4.6\%$. Addition of oligomycin inhibited ATP production by about 95% indicating that most of the ATP production could be attributed to oxidative phosphorylation.

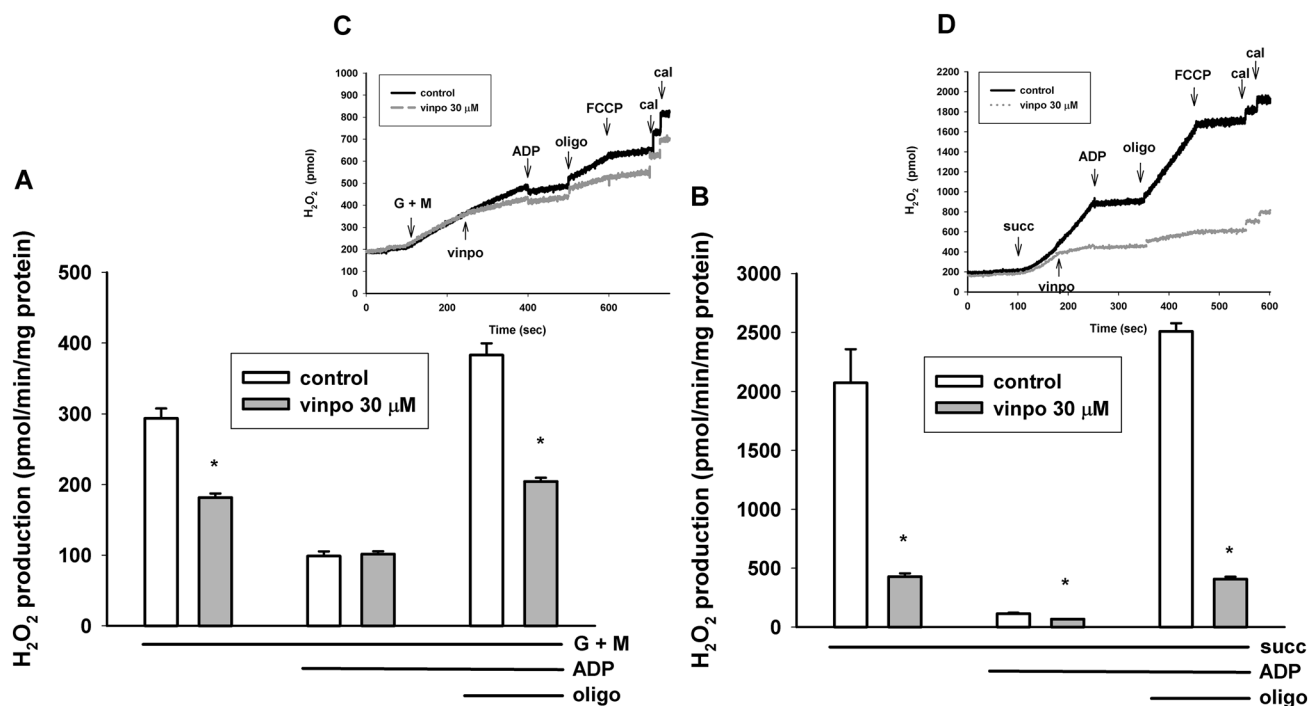


Fig. 7 Effects of vinpocetine on mitochondrial H_2O_2 formation in glutamate *plus* malate (a) and succinate-supported (b) mitochondria. Mitochondria were incubated in the standard mitochondrial medium. Vinpocetine (vinpo; 30 μM), ADP (2 mM), oligomycin (oligo;

5 μM), and FCCP (250 nM) were given as indicated in the insets. At the end of each measurement 100 pmol H_2O_2 was added for calibration (cal). * indicates significant difference ($p < 0.05$, $n > 4$) from the corresponding vinpocetine-free controls

ATPase Activity of Mitochondria

The formation of ATP by oxidative phosphorylation is influenced by many factors, e.g. transport of respiratory substrates, ADP, activity of respiratory complexes, activity of citric acid cycle enzymes. Therefore, for specific assessment of ATP synthase activity mitochondria were supported by ATP only and the rate of mitochondrial ADP release was measured. Mitochondria were incubated in the presence of vinpocetine (30 μM) or vehicle. In the presence of vinpocetine the rate of ADP hydrolysis more than doubled (increased by 137%). The uncoupler FCCP stimulated ADP hydrolysis and mitigated the difference between the effect of vinpocetine. In order to detect the maximal reverse activity of ATP synthase, mitochondria were permeabilized by the pore forming alamethicin. Vinpocetine also stimulated ATP hydrolysis in fully permeabilized mitochondria (Fig. 8b).

Mitochondrial Ca^{2+} Uptake and Ca^{2+} -Induced Ca^{2+} Release

Another function of mitochondria is Ca^{2+} -handling. To assess the Ca^{2+} uptake capacity, Ca^{2+} pulses (12.5 μM) were added and taken up by the mitochondria in 50 s intervals (Fig. 9a). The uptake was fast (V_{max} for the Ca^{2+} uniporter was 1200 nmol Ca^{2+} /min/mg protein. After adding multiple

Ca^{2+} pulses, the Ca^{2+} uptake capacity of mitochondria was gradually lost. When Ca^{2+} uptake stopped, mitochondria started to release the previously accumulated Ca^{2+} due to the mPTP opening (Ca^{2+} -induced Ca^{2+} release (mCICR)). In the presence of vinpocetine (30 μM), the maximal Ca^{2+} uptake capacity of mitochondria remained unaltered, however the mCICR decreased.

Effect of Vinpocetine on Ca^{2+} -Induced Swelling of Mitochondria

In the above mCICR assay, in parallel with Ca^{2+} recording, swelling of mitochondria was measured from the same samples (Fig. 9b). In the presence of vinpocetine (30 μM) mitochondrial swelling (an indicator of mPTP opening) was decreased, indicated by the smaller decrease in light scatter after the onset of mCICR.

Discussion

Vinpocetine was introduced to clinical therapy decades ago, and many possible molecules and structures were associated as targets for its beneficial effects. It is obvious that energy homeostasis is a crucial factor in the cell survival and can

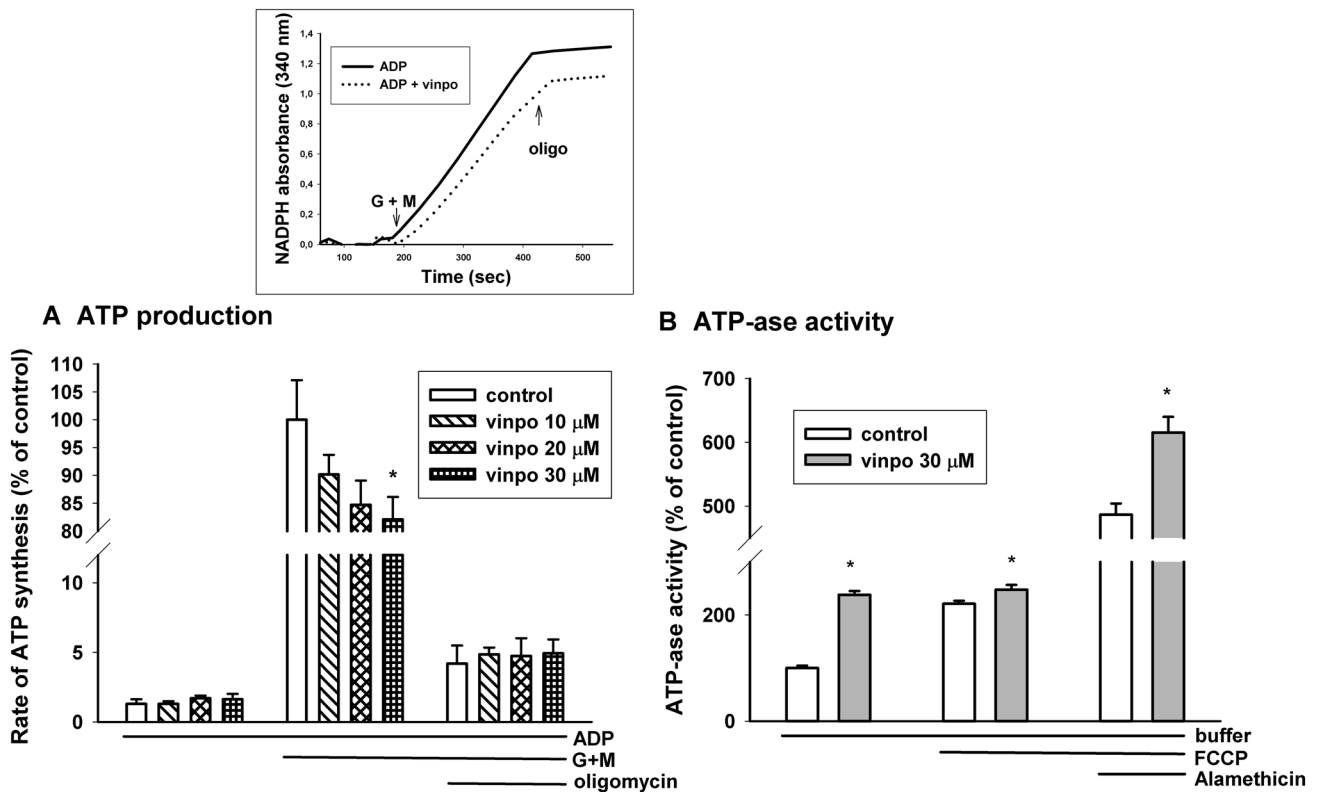


Fig. 8 Effects of vinpocetine on mitochondrial ATP synthesis (a) and ATPase activity (b). The rate of ATP synthesis in glutamate plus malate (G+M) supported mitochondria (0.5 mg/ml mitochondrial protein was measured in standard medium supplemented with the inhibitor of adenylate kinase, ADP (2 mM) in the presence (hatched bars on (a) and dotted line on the inset) or absence (white bars on (a), solid line on the inset) of vinpocetine. At 200 s G+M initiated oxidative substrate-dependent ATP synthesis. Oligomycin (oligo; 5 μM)

inhibited oxidative phosphorylation. ATPase activity (b) was measured on the basis of hydrolysis of exogenous ATP given to mitochondria. ATP hydrolysis was measured under resting conditions (buffer), in the presence of uncoupler FCCP (250 nM) and in the presence of alamethicin, a pore-forming antibiotics. Vinpocetine (vinpo; 30 μM; gray bars). * indicates significant difference ($p < 0.05$, $n > 4$) from the corresponding vinpocetine-free controls (white bars)

also determine the type of cell death. Although the binding of vinpocetine to the mitochondrial peripheral benzodiazepine receptor (PBR) has already been demonstrated [41, 42], systematic mitochondrial studies have not followed this early observation.

In the present study, the bioenergetic aspects of the effects of vinpocetine were investigated on primary brain capillary endothelial cells, neurons, isolated nerve terminals (synaptosomes) and in isolated mitochondria.

Measurements in Cellular Systems

Ca²⁺ Transients in Primary Brain Capillary Endothelial Cells

Integrity of the blood brain barrier is an important factor in the maintenance of CNS homeostasis [43]. In brain capillary endothelial cells, purinergic signaling evoked cytoplasmic

and mitochondrial Ca²⁺ transients (Fig. 1). In the presence of vinpocetine the peak height of the Ca²⁺ transient remained unaltered, however, the half decay time of the mitochondrial Ca²⁺ transient was increased, thus Ca²⁺ release was slower in the presence of vinpocetine (Fig. 2). The phenomenon may be attributed to inhibition of the mitochondrial Na⁺/Ca²⁺ exchange, the major route of the mitochondrial Ca²⁺ release [44]. This effect of vinpocetine is similar to that found with CGP-37157, a dedicated inhibitor of the mitochondrial Na⁺-dependent Ca²⁺ release [25]. CGP-37157 has neuroprotective effects [45]. Inhibition of ion channels is also in the spectrum of vinpocetine, e.g. it is an efficient blocker of the tetrodotoxin-sensitive voltage dependent Na⁺ channel. Nevertheless, there are further alternative explanations. Depolarization of mitochondria decreases the driving force of transport processes including the energy required for the forward operation of the Na⁺/Ca²⁺ exchanger [46].

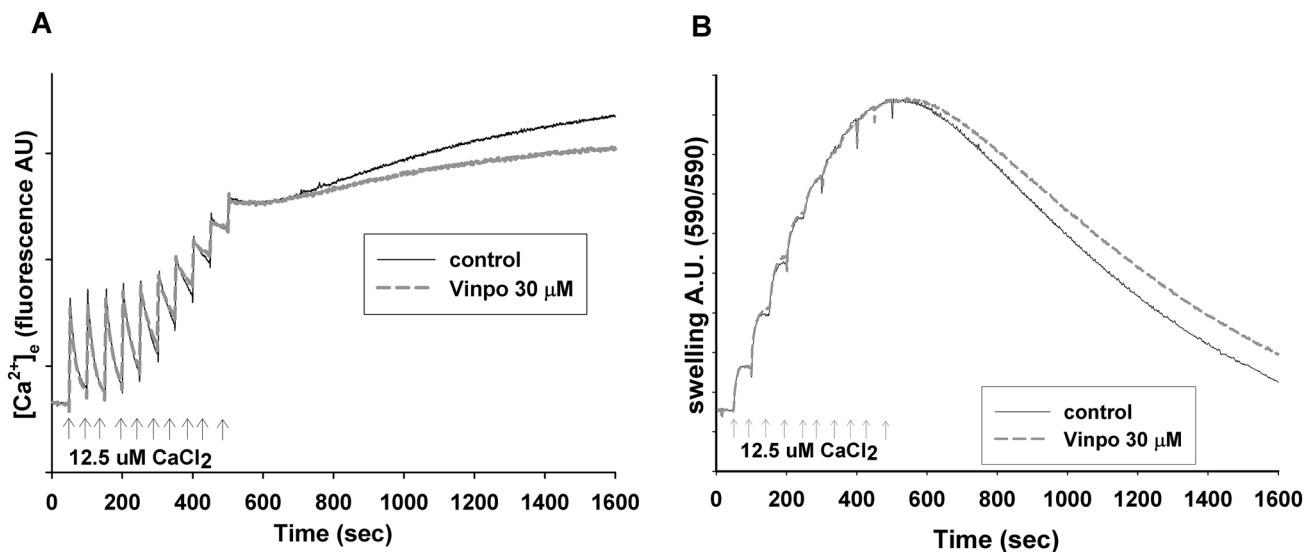


Fig. 9 Effect of vinpocetine on mitochondrial Ca^{2+} handling. Effect of vinpocetine on the Ca^{2+} uptake capacity and mCICR. **a** Rat brain mitochondria (0.05 mg/ml) were incubated in reaction medium. $CaCl_2$ pulses were added as indicated. The free $[Ca^{2+}]_e$ of the medium was detected by Calcium-Green 5 N fluorescence in the absence (control) or in the presence of vinpocetine (vinpo, 30 μM) as indicated.

Delayed Ca^{2+} Deregulation (DCD) in Cortical Neurons

DCD is a model of glutamate toxicity, where excessive Ca^{2+} loads through Ca^{2+} permeable glutamate channels could result in deterioration of calcium and energy homeostasis. Vinpocetine did not affect DCD in primary cortical neurons. Our results somewhat differ from those published by others [12]. The reason of discrepancy is possibly attributed to the higher glutamate concentration applied in the present study (300 μM for 20 min vs. 25 μM for 30 min).

Measurements on Isolated Nerve Terminals (Synaptosomes)

Oxygen Consumption Measurements

Oxygen consumption of synaptosomes is attributed to the substrate oxidation of in situ mitochondria [47]. Thus, glucose used as an energy supply for synaptosomes is metabolised in glycolysis and subsequently in the mitochondria. Compromised mitochondrial O_2 consumption in synaptosomes energized by external glucose (Fig. 4) could be also explained by inhibition of either the glucose transport or glycolysis, besides mitochondrial effects. In order to rule out these possibilities, lactate was also used as respiratory substrate. Vinpocetine inhibited synaptosomal O_2 consumption similarly in the presence of glucose or lactate, ruling out

The loss of Ca^{2+} buffering capacity is followed by mCICR. Representative traces $n > 3$. Calcium induced swelling of mitochondria (**b**). Swelling of mitochondrial matrix was measured simultaneously with Ca^{2+} uptake by the light scattering method. More that swelling and the loss of Ca^{2+} buffering capacity were developed at the same time. Representative traces $n > 3$ from independent experiments

that this inhibition was be specific to the glucose metabolism. These observations directed our attention towards isolated mitochondria.

Release of H_2O_2 from Synaptosomes

Vinpocetine inhibited H_2O_2 formation in synaptosomes. Measurement of synaptosomal H_2O_2 production using Amplex Ultrared dye and horseradish peroxidase gives indirect information about the ROS homeostasis. The information are indirect, because (i) ROS sources other than mitochondria e.g. NADPH oxidases [47, 48], and nitrogen monoxide synthase (NOS) [49] can also be found in synaptosomes (ii) the cytoplasm possesses many enzymatic and nonenzymatic ROS scavenging systems [50, 51] and our detection system for H_2O_2 is extra-synaptosomal; in synaptosomes between the mitochondrial membranes and the plasma membrane of the synaptosomes both ROS generating and scavenging mechanisms can be found, therefore more direct information was acquired using isolated mitochondria.

Measurements in Isolated Guinea Pig Brain Mitochondria

Effect of Vinpocetine on Mitochondrial Membrane Potential, Oxygen Consumption and H_2O_2 Formation

In isolated mitochondria membrane potential was slightly depolarized (4.0 ± 0.6 mV) by vinpocetine. This together

with an increased respiration in the absence of ADP (Fig. 6) suggests an uncoupler-like effect that could be detected with both glutamate *plus* malate and succinate as respiratory substrates. In the absence of ADP (substrate only conditions) or in the presence of oligomycin the mitochondrial membrane potential is high and redox centers are very reduced. In this condition a high rate of H₂O₂ production was detected both with complex I and complex II substrates (Fig. 7). Even slight depolarization could exponentially decrease the ROS formation under these conditions [40, 52, 53]. Therefore, the ROS lowering effect of vinpocetine may be explained by mild uncoupling. The ADP stimulated respiration was strongly inhibited in the presence of vinpocetine. Like the depolarization in ADP-free conditions, the respiratory inhibition was also independent from what type of substrates (complex I or complex II) supported the mitochondria. This finding raises the possibility that either both complex I and II, or complex III, or complex IV or their combination were inhibited by vinpocetine.

ATP Synthetic and ATP Hydrolytic Rates in the Presence of Vinpocetine

Vinpocetine decreased the rate of ATP synthesis with glutamate *plus* malate as respiratory substrates, but increased the rate of ATP hydrolysis in the absence of respiration-supporting substrates. The concrete reasons behind a compromised mitochondrial ATP synthesis is generally rather obscure. In order to produce ATP efficiently, tens of mechanisms behind the four postulates of Mitchell should work perfectly and in synchrony. It is rather difficult to evaluate our findings from the aspect of neuroprotection. The slight decrease in the rate of ATP synthesis in the presence of vinpocetine might be attributed to the uncoupling detected in O₂ consumption measurements. A less efficient ATP synthesis is not beneficial from the point of cell survival. On the other hand, an uncoupling-evoked decrease in membrane potential would decrease the rate of ROS production and could also accelerate ROS elimination by stimulating NADPH formation via the NADP⁺-dependent isocitrate dehydrogenase or glutamate dehydrogenase. Therefore, this phenomenon might improve the redox homeostasis in mitochondria and the cell. The increased ATP hydrolysis rate suggests that vinpocetine does not inhibit the reverse mode of ATP synthase (and perhaps does not inhibit its forward mode, either).

Seeking the Mechanism and Conclusions

In the present paper, we attempted to describe the effects of vinpocetine on selected mitochondrial functions in light of

the well documented beneficial effects of the drug on brain functions. Various findings presented above are somewhat controversial. Some of them may first seem to be negative, e.g. inhibition of mitochondrial respiration and ATP synthesis. Some of the effects are subjects of various interpretations, e.g. mild uncoupling (its benefits are debated), the increased half time of Ca²⁺ release from endothelial cells, the possible inhibition of the mitochondrial Na⁺/Ca²⁺ exchanger, all may or may not have beneficial physiological effects. Finally, inhibition of the Ca²⁺-induced mitochondrial swelling, delayed CICR, and the very strong inhibition of the mitochondrial H₂O₂ release are all unequivocally positive.

Considering that vinpocetine does not display any severe side effects, we may conclude that the positive effects dominate under *in vivo* conditions. We also conclude that on the basis of the results presented above it is very likely that vinpocetine possesses more than one molecular target in mitochondria.

Acknowledgement Open access funding provided by Semmelweis University (SE). Authors are indebted to Christos Chinopoulos (Semmelweis University) for helping us in Ca²⁺ handling experiments on isolated mitochondria. Authors are also grateful to Katalin Takacs and Andrea Varnagy for the excellent technical assistance. This work was supported by the Hungarian Brain Research Program (KTIA_13_NAP-A-III/6 and 2017-1.2.1-NKP-2017-00002), OTKA (K 112230), Hungarian Higher Education Institution Excellence Program [FIKP 61822 64860 EATV and FIKP 61826 690289 EATV] and the Hungarian Academy of Sciences (MTA TKI 02001), all to Vera Adam-Vizi.

Compliance with Ethical Standards

Conflict of interest Part of this work was supported by the Gedeon Richter Plc. AAG has financial interest in Image Analyst Software.

Open Access This article is distributed under the terms of the Creative Commons Attribution 4.0 International License (<http://creativecommons.org/licenses/by/4.0/>), which permits unrestricted use, distribution, and reproduction in any medium, provided you give appropriate credit to the original author(s) and the source, provide a link to the Creative Commons license, and indicate if changes were made.

References

1. Nivison-Smith L, O'Brien BJ, Truong M, Guo CX, Kalloniatis M, Acosta ML (2015) Vinpocetine modulates metabolic activity and function during retinal ischemia. *Am J Physiol Cell Physiol* 308:C737–C749
2. Bonoczk P, Panczel G, Nagy Z (2002) Vinpocetine increases cerebral blood flow and oxygenation in stroke patients: a near infrared spectroscopy and transcranial Doppler study. *Eur J Ultrasound* 15:85–91
3. Szobor A, Klein M (1992) Examinations of the relative fluidity in cerebrovascular disease patients. *Ther Hung* 40:8–11
4. Rischke R, Krieglstein J (1991) Protective effect of vinpocetine against brain damage caused by ischemia. *Jpn J Pharmacol* 56:349–356

5. Medina AE (2011) Therapeutic utility of phosphodiesterase type I inhibitors in neurological conditions. *Front Neurosci* 5:21
6. Heckman PR, Wouters C, Prickaerts J (2015) Phosphodiesterase inhibitors as a target for cognition enhancement in aging and Alzheimer's disease: a translational overview. *Curr Pharm Des* 21:317–331
7. Paroczai M, Kiss B, Karpati E (1998) Effect of RGH-2716 on learning and memory deficits of young and aged rats in water-labyrinth. *Brain Res Bull* 45:475–488
8. Chiu PJ, Tetzloff G, Ahn HS, Sybertz EJ (1988) Comparative effects of vinpocetine and 8-Br-cyclic GMP on the contraction and ^{45}Ca -fluxes in the rabbit aorta. *Am J Hypertens* 1:262–268
9. Hagiwara M, Endo T, Hidaka H (1984) Effects of vinpocetine on cyclic nucleotide metabolism in vascular smooth muscle. *Biochem Pharmacol* 33:453–457
10. Erdo SA, Molnar P, Lakics V, Bence JZ, Tomoskozi Z (1996) Vincamine and vincanol are potent blockers of voltage-gated Na^+ channels. *Eur J Pharmacol* 314:69–73
11. Tretter L, Adam-Vizi V (1998) The neuroprotective drug vinpocetine prevents veratridine-induced $[\text{Na}^+]_i$ and $[\text{Ca}^{2+}]_i$ rise in synaptosomes. *NeuroReport* 9:1849–1853
12. Jeon KI, Xu X, Aizawa T, Lim JH, Jono H, Kwon DS, Abe J, Berk BC, Li JD, Yan C (2010) Vinpocetine inhibits NF- κ B-dependent inflammation via an IKK-dependent but PDE-independent mechanism. *Proc Natl Acad Sci USA* 107:9795–9800
13. Tarnok K, Kiss E, Luiten PG, Nyakas C, Tihanyi K, Schlett K, Eisel UL (2008) Effects of Vinpocetine on mitochondrial function and neuroprotection in primary cortical neurons. *Neurochem Int* 53:289–295
14. Zhang YS, Li JD, Yan C (2018) An update on vinpocetine: new discoveries and clinical implications. *Eur J Pharmacol* 819:30–34
15. Andreyev AY, Kushnareva YE, Starkov AA (2005) Mitochondrial metabolism of reactive oxygen species. *Biochemistry (Moscow)* 70:200–214
16. Torres-Cuevas I, Corral-Debrinski M, Gressens P (2019) Brain oxidative damage in murine models of neonatal hypoxia/ischemia and reoxygenation. *Free Radic Biol Med*
17. Starkov AA, Chinopoulos C, Fiskum G (2004) Mitochondrial calcium and oxidative stress as mediators of ischemic brain injury. *Cell Calcium* 36:257–264
18. Love S (1999) Oxidative stress in brain ischemia. *Brain Pathol* 9:119–131
19. Halliwell B (1992) Reactive oxygen species and the central nervous system. *J Neurochem* 59:1609–1623
20. Dumont M, Beal MF (2011) Neuroprotective strategies involving ROS in Alzheimer disease. *Free Radic Biol Med* 51:1014–1026
21. Nicholls DG (2009) Mitochondrial calcium function and dysfunction in the central nervous system. *Biochim Biophys Acta* 1787:1416–1424
22. Gulyas B, Toth M, Vas A, Shchukin E, Kostulas K, Hillert J, Halldin C (2012) Visualising neuroinflammation in post-stroke patients: a comparative PET study with the TSPO molecular imaging biomarkers $[\text{11C}]\text{PK11195}$ and $[\text{11C}]\text{vinpocetine}$. *Curr Radiopharm* 5:19–28
23. Domotor E, Abbott NJ, Adam-Vizi V (1999) Na^+ - Ca^{2+} exchange and its implications for calcium homeostasis in primary cultured rat brain microvascular endothelial cells. *J Physiol* 515(Pt 1):147–155
24. Chinopoulos C, Gerencser AA, Doczi J, Fiskum G, Adam-Vizi V (2004) Inhibition of glutamate-induced delayed calcium deregulation by 2-APB and La^{3+} in cultured cortical neurones. *J Neurochem* 91:471–483
25. Gerencser AA, Adam-Vizi V (2001) Selective, high-resolution fluorescence imaging of mitochondrial Ca^{2+} concentration. *Cell Calcium* 30:311–321
26. Hajos F (1975) An improved method for the preparation of synaptosomal fractions in high purity. *Brain Res* 93:485–489
27. Sims NR (1990) Rapid isolation of metabolically active mitochondria from rat brain and subregions using Percoll density gradient centrifugation. *J Neurochem* 55:698–707
28. Tretter L, Adam-Vizi V (2007) Moderate dependence of ROS formation on DeltaPsim in isolated brain mitochondria supported by NADH-linked substrates. *Neurochem Res* 32:569–575
29. Gnaiger E (2001) Bioenergetics at low oxygen: dependence of respiration and phosphorylation on oxygen and adenosine diphosphate supply. *Respir Physiol* 128:277–297
30. Kamo N, Muratsugu M, Hongoh R, Kobatake Y (1979) Membrane potential of mitochondria measured with an electrode sensitive to tetraphenyl phosphonium and relationship between proton electrochemical potential and phosphorylation potential in steady state. *J Membr Biol* 49:105–121
31. Tretter L, Adam-Vizi V (2007) Moderate dependence of ROS formation on DeltaPsim in isolated brain mitochondria supported by NADH-linked substrates. *Neurochem Res* 32:569–575
32. Schoenmakers TJ, Visser GJ, Flik G, Theuvsen AP (1992) CHE-LATOR: an improved method for computing metal ion concentrations in physiological solutions. *Biotechniques* 12:870–879
33. Gunter TE, Pfeiffer DR (1990) Mechanisms by which mitochondria transport calcium. *Am J Physiol* 258:C755–C786
34. Zoratti M, Szabo I (1995) The mitochondrial permeability transition. *Biochim Biophys Acta* 1241:139–176
35. Komlodi T, Tretter L (2017) Methylene blue stimulates substrate-level phosphorylation catalysed by succinyl-CoA ligase in the citric acid cycle. *Neuropharmacology* 123:287–298
36. Williamson JR, Corkey BE (1979) Assay of citric acid cycle intermediates and related compounds—update with tissue metabolite levels and intracellular distribution. *Methods Enzymol* 55:200–222
37. Teruel JA, Tudela J, Fernandez-Belda F, Garcia-Carmona F, Garcia-Canovas F, Gomez-Fernandez JC (1986) A kinetic study of the irreversible inhibition of an enzyme measured in the presence of coupled enzymes. Fluorescein isothiocyanate as inhibitor of the adenosinetriphosphatase activity from sarcoplasmic reticulum. *Biochim Biophys Acta* 869:8–15
38. Nicholls DG, Johnson-Cadwell L, Vesce S, Jekabsons M, Yadava N (2007) Bioenergetics of mitochondria in cultured neurons and their role in glutamate excitotoxicity. *J Neurosci Res* 85:3206–3212
39. Komary Z, Tretter L, Adam-Vizi V (2008) H_2O_2 generation is decreased by calcium in isolated brain mitochondria. *Biochim Biophys Acta* 1777:800–807
40. Starkov AA, Polster BM, Fiskum G (2002) Regulation of hydrogen peroxide production by brain mitochondria by calcium and Bax. *J Neurochem* 83:220–228
41. Gulyas B, Halldin C, Vas A, Banati RB, Shchukin E, Finnema S, Tarkainen J, Tihanyi K, Szilagyi G, Farde L (2005) $[\text{11C}]\text{vinpocetine}$: a prospective peripheral benzodiazepine receptor ligand for primate PET studies. *J Neurol Sci* 229–230:219–223
42. Vas A, Shchukin Y, Karrenbauer VD, Cselenyi Z, Kostulas K, Hillert J, Savic I, Takano A, Halldin C, Gulyas B (2008) Functional neuroimaging in multiple sclerosis with radiolabelled gliamarkers: preliminary comparative PET studies with $[\text{11C}]\text{vinpocetine}$ and $[\text{11C}]\text{PK11195}$ in patients. *J Neurol Sci* 264:9–17
43. Abbott NJ, Patabendige AA, Dolman DE, Yusof SR, Begley DJ (2010) Structure and function of the blood-brain barrier. *Neurobiol Dis* 37:13–25
44. Hoppe UC (2010) Mitochondrial calcium channels. *FEBS Lett* 584:1975–1981
45. Garcia-Casas P, Arias-Del-Val J, Alvarez-Illera P, Wojnicz A, de Los RC, Fonteriz RI, Montero M, Alvarez J (2018) The

- neuroprotector benzothiazepine CGP37157 extends lifespan in *C. elegans* worms. *Front Aging Neurosci* 10:440
46. Kim B, Matsuoka S (2008) Cytoplasmic Na⁺-dependent modulation of mitochondrial Ca²⁺ via electrogenic mitochondrial Na⁺-Ca²⁺ exchange. *J Physiol* 586:1683–1697
 47. Abdel-Rahman EA, Mahmoud AM, Aaliya A, Radwan Y, Yasseen B, Al-Okda A, Atwa A, Elhanafy E, Habashy M, Ali SS (2016) Resolving contributions of oxygen-consuming and ROS-generating enzymes at the synapse. *Oxid Med Cell Longev* 2016:1089364
 48. Valencia A, Sapp E, Kimm JS, McClory H, Reeves PB, Alexander J, Ansong KA, Masso N, Frosch MP, Kegel KB, Li X, DiFiglia M (2013) Elevated NADPH oxidase activity contributes to oxidative stress and cell death in Huntington's disease. *Hum Mol Genet* 22:1112–1131
 49. Alekseenko AV, Lemeshchenko VV, Pekun TG, Waseem TV, Fedorovich SV (2012) Glutamate-induced free radical formation in rat brain synaptosomes is not dependent on intrasynaptosomal mitochondria membrane potential. *Neurosci Lett* 513:238–242
 50. Bizzozero OA, Ziegler JL, De JG, Bolognani F (2006) Acute depletion of reduced glutathione causes extensive carbonylation of rat brain proteins. *J Neurosci Res* 83:656–667
 51. Cardoso SM, Pereira C, Oliveira CR (1998) The protective effect of vitamin E, idebenone and reduced glutathione on free radical mediated injury in rat brain synaptosomes. *Biochem Biophys Res Commun* 246:703–710
 52. Korshunov SS, Skulachev VP, Starkov AA (1997) High protonic potential actuates a mechanism of production of reactive oxygen species in mitochondria. *FEBS Lett* 416:15–18
 53. Miwa S, St-Pierre J, Partridge L, Brand MD (2003) Superoxide and hydrogen peroxide production by *Drosophila* mitochondria. *Free Radic Biol Med* 35:938–948

Publisher's Note Springer Nature remains neutral with regard to jurisdictional claims in published maps and institutional affiliations.